Journal of the Optical Society of Korea
Vol. 19, No. 6, December 2015, pp. 705-710

ISSN: 1226-4776(Print) / ISSN: 2093-6885(Online)
DOI: http://dx.doi.org/10.3807/JOSK.2015.19.6.705

Opto-Electrochemical Sensing Device Based on Long-Period Grating Coated with Boron-Doped Diamond Thin Film

Robert Bogdanowicz[1], Michał Sobaszek[1], Mateusz Ficek[1], Marcin Gnyba[1], Jacek Ryl[2], Katarzyna Siuzdak[3], Wojtek J. Bock[4], and Mateusz Śmietana[5]*

[1]Department of Metrology and Optoelectronics, Faculty of Electronics, Telecommunications and Informatics, Gdansk University of Technology, Narutowicza 11/12, 80-233 Gdansk, Poland
[2]Department of Electrochemistry, Corrosion and Material Engineering, Gdansk University of Technology, Narutowicza 11/12, 80-233 Gdansk, Poland
[3]Centre for Plasma and Laser Engineering, The Szewalski Institute of Fluid-Flow Machinery, Polish Academy of Sciences, Fiszera 14, 80-231 Gdansk, Poland
[4]Centre de Recherche en Photonique, Université du Québec en Outaouais, 101 Rue Saint-Jean-Bosco, Gatineau, QC J8X 3X7, Canada
[5]Institute of Microelectronics and Optoelectronics, Warsaw University of Technology, Koszykowa 75, 00-662 Warszawa, Poland

(Received August 4, 2015 : revised November 2, 2015 : accepted November 2, 2015)

The fabrication process of thin boron-doped nanocrystalline diamond (B-NCD) microelectrodes on fused silica single mode optical fiber cladding has been investigated. The B-NCD films were deposited on the fibers using Microwave Plasma Assisted Chemical Vapor Deposition (MW PA CVD) at glass substrate temperature of 475 ºC. We have obtained homogenous, continuous and polycrystalline surface morphology with high sp^3 content in B-NCD films and mean grain size in the range of 100-250 nm. The films deposited on the glass reference samples exhibit high refractive index (n=2.05 at λ=550 nm) and low extinction coefficient. Furthermore, cyclic voltammograms (CV) were recorded to determine the electrochemical window and reaction reversibility at the B-NCD fiber-based electrode. CV measurements in aqueous media consisting of 5 mM $K_3[Fe(CN)_6]$ in 0.5 M Na_2SO_4 demonstrated a width of the electrochemical window up to 1.03 V and relatively fast kinetics expressed by a redox peak splitting below 500 mV. Moreover, thanks to high-n B-NCD overlay, the coated fibers can be also used for enhancing the sensitivity of long-period gratings (LPGs) induced in the fiber. The LPG is capable of measuring variations in refractive index of the surrounding liquid by tracing the shift in resonance appearing in the transmitted spectrum. Possible combined CV and LPG-based measurements are discussed in this work.

Keywords : Boron-doped nanocrystalline diamond, Thin films, Optical constants, Fiber optical sensors, Long-period grating
OCIS codes : (310.0310) Thin films; (120.4530) Optical constants; (060.2370) Fiber optics sensors; (350.2770) Gratings

I. INTRODUCTION

Investigations of optical and chemical properties are currently in high demand for medical diagnostics and biochemical analysis. Optical-fiber-based sensors, e.g., refractometers, where refractive index (RI) is investigated, gained a lot of attention due to their possible probe-like shape, repeatable and low cost fabrication of the optical fibers and their interrogation systems, which are well-developed for telecommunication [1]. Long-period gratings (LPGs) have been known for over a decade [2]. LPGs are periodic modulations of the refractive index in fiber core along the length of a fiber. Under certain phase-matching conditions, the grating couples the fundamental core mode and discrete cladding modes

*Corresponding author: m.smietana@elka.pw.edu.pl
Color versions of one or more of the figures in this paper are available online.

that are attenuated due to absorption and scattering. The coupling is wavelength-dependent, so one can obtain a spectrally selective loss. A number of sensors based on the LPGs have been proposed for temperature, humidity, strain, hydrostatic pressure, bending and RI sensing, including a number of biosensors [3-6].

It has also been shown that the deposition of some overlays can significantly modify sensitivity of LPG structures to certain external influences. Deposition of the high-refractive-index (high-*n*) nano-coatings [7-9], which include diamond-like carbon overlays [10], may significantly increase sensitivity of the LPG structures to variations in external RI. Such coatings make it possible to optimize the interactions of the light guided in the fiber and in the coating, resulting in enhancing intrinsic sensitivity of optical fiber devices to a certain range of the measured quantity. Most of the nano-coatings presented to date exhibit dielectric properties. Corres *et al*. showed humidity sensors based on LPG with two-layer nano-coatings [7]. The authors proposed application of electrostatic self-assembled alumina (Al_2O_3) and poly (sodium 4-sterenesulfonate) for enhancing sensitivity to external RI. Davies *et al.* showed sol-gel based coatings of silicon (SiO_2) and titanium (TiO_2) oxides also for improving the detection of RI changes [8]. Nano-coated LPGs allow for detection for changes of RI as small as 10^{-5} in solution samples.

Diamond is a wide band gap semiconductor with E_g = 5.45 eV. It can be easily doped with boron using an *in situ* Chemical Vapor Deposition (CVD) process. Due to the presence of boron, diamond effectively changes its electrical conductivity and becomes a p-type semiconductor. Boron nanocrystalline diamond (B-NCD) films exhibit a set of remarkable properties, which include biocompatibility, optical transparency in broad wavelength [11] and electro-chemical features, i.e., chemical stability [12, 13], a wide electrochemical window and high anodic stability. B-NCD films appear to be a promising material for optically transparent electrodes in opto-electrochemical devices [14].

In this paper we analyze several cm long optical fiber sections coated with B-NCD overlay using the Microwave Plasma Assisted Chemical Vapor Deposited (MW PA CVD) method. The work focuses on investigation of overlay properties and application of the coated device for both optical and electrochemical investigations of liquids.

II. EXPERIMENTAL DETAILS

Fabrication procedure of LPGs with computer-assisted precision arc-discharge apparatus has been described previously in [15]. In this stage of the experiment, we used Corning SMF28 fiber samples to write gratings with period of Λ = 500 μm.

Fibers were nucleated by means of dip-coating in dispersion consisting of detonation nanodiamond (DND) in dimethyl sulfoxide (DMSO) with polyvinyl alcohol (PVA). Next, the B-NCD films were deposited on the fibers using an MW PA CVD system (SEKI Technotron). The deposition process took 60 minutes with the total flow rate of gases reaching 300 sccm at methane molar ratio of 4% and 5000 ppm [B]/[C] ratio in gas phase. The holder temperature was 475 °C and process pressure was kept at 50 Torr.

The morphological studies were performed with a Hitachi S-3400N scanning electron microscope (SEM). The molecular composition of the films was studied by means of Raman spectroscopy using a Horiba LabRAM ARAMIS Raman confocal microscope. Spectroscopic ellipsometry (SE) investi-gations on reference Si samples were carried out with a Horiba Jobin-Yvon UVISEL phase-modulated ellipsometer [16].

Furthermore, cyclic voltammograms (CV) were recorded to determine the electrochemical window and reaction reversibility at the B-NCD fiber-based electrode. CV measurements were performed in aqueous media consisting of 5 mM $K_3[Fe(CN)_6]$ in 0.5 M Na_2SO_4 at scan rate of 0.1 V s^{-1}. The electro-chemical system includes three electrodes, i.e., B-NCD-coated fiber, Ag/AgCl/0.1 M KCl and platinum wire as working, reference and counter electrodes, respectively. The electrochemical experiment was performed using an Autolab PGSTAT30 system.

Next, the transmission of the LPG samples was measured in wavelength range 1150 to 1650 nm using a Yokogawa AQ4305 white light source and Yokogawa AQ6370B optical spectrum analyzer. For the RI measurements, the nano-coated LPG was immersed in various liquids prepared by mixing water and glycerin. The RI of the obtained liquid (n_D) was measured using Reichert AR200 Refractometer with accuracy +/-10^{-4} RI units (RIU).

III. RESULTS AND DISCUSSION

As a result of SE analysis performed on B-NCD-coated Si reference samples, the thickness and optical constants of diamond film, i.e. refractive index $n(\lambda)$ and extinction coefficient $k(\lambda)$ dispersion curves were obtained (Fig. 1(a)). The optical constants of B-NCD films decrease with wavelength, exhibiting a typical behavior near the band gap of electronic transition. The n reaches 2.05 at λ=550 nm and about 2 in IR spectral range, thus the material shows higher n than for fused silica glass and is capable of tuning the response of a number of optical-fiber-based sensing devices [17-19]. Nevertheless, the obtained values of n are smaller than those for the single-crystal diamond (2.41) [20]. This effect is related to decrease in the sp^3/sp^2 carbon phase ratio when nanocrystalline films are deposited [21]. Moreover, it can be seen that k increases with wavelength in its range above 350 nm. This can be explained by the sp^2 bond content and intensive boron incorporation at the interface between the grains [22].

Fiber cross-sections reveal no significant change, i.e., dopant diffusion, in the fiber core after high-temperature B-NCD film deposition (Fig. 2(a)). The obtained diamond

overlay is continuous and homogenous along the fiber (Fig. 2(b)), in agreement with previously obtained results on the fused glass slides [23, 24]. Average crystallite size is between 100 and 200 nm (Fig. 3(b)) and thickness of the films is below 500 nm. A deposition rate of 10 nm/min was reached.

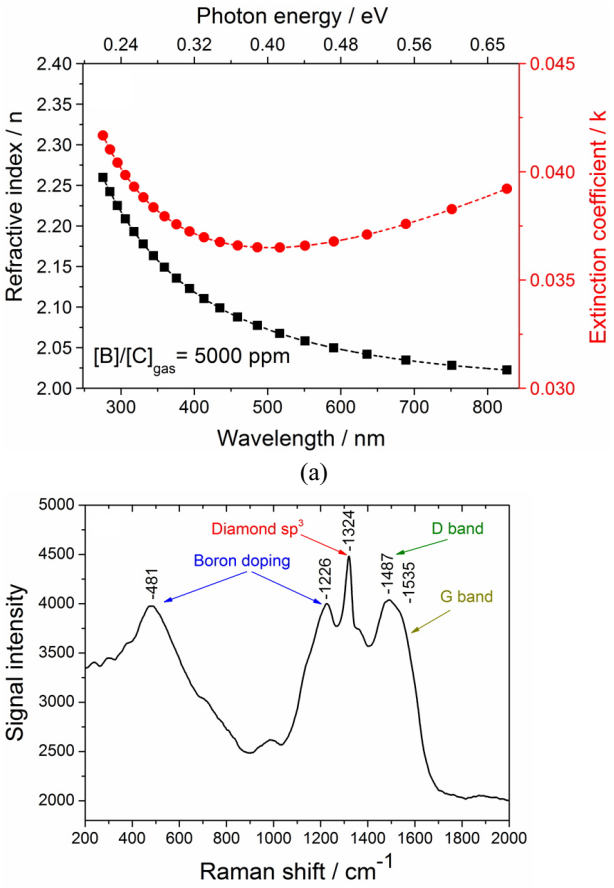

FIG. 1. Properties of the B-NCD films, where (a) shows dispersion of *n* and *k*, and (b) presents Raman spectrum of the film deposited on the fused silica fiber surface.

Raman spectrum shown in Fig. 1(b) proves the presence of strong bands assigned to the diamond lattice, and confirms a high content of sp^3 carbon in the film structure. Its shift from typical for diamond 1330 to about 1324 cm^{-1} is caused by a stress introduced by boron doping [25]. Moreover, the boron presence in the sample can be confirmed by a band observed at 1226 cm^{-1} and by a strong signal intensity drop above 1650 cm^{-1}. The D band at 1487 cm^{-1} can be assigned to the mixture of amorphous carbon phase sp^2 and sp^3, while the G band at 1535 cm^{-1}, to sp^2-bonded amorphous carbon.

The effect of the B-NCD overlay deposition on LPG response to external RI is shown in Fig. 3. As shown for RI close to that of water (n_D=1.333) where most of the biosensors operate, the deposition process had significant influence on LPG resonance, i.e., decrease in depth and their spectral shift towards shorter wavelengths (Fig. 3(a)). The change in response induced by the deposition process when compared to a bare LPG sample can be attributed to both high temperature of the process and B-NCD overlay deposition [26]. The decrease in depth results from the temperature-induced decrease in refractive index modulation in fiber core at the LPG region. For the B-NCD deposition, the temperature at the fiber can locally reach 550 ºC. The distribution of temperature along the fiber is mostly driven by density of the microwave power. The fused silica is transparent at microwave frequencies as well as to infrared radiation generated by the induction heater. Thus, local changes in temperatures are induced mainly by conduction heat transfer phenomenon and different parts of the fiber can be heated differently at the deposition stage. What is more, different values of thermal expansion coefficient of polycrystalline diamond film and the amorphous fused silica substrate also have an influence also on deposition-induced strain effect. However, both the processes exhibit nanothermomechanic character and cannot be controlled or measured locally due to high temperature and ionic plasma character. Previously presented micromorphological SEM studies [27]

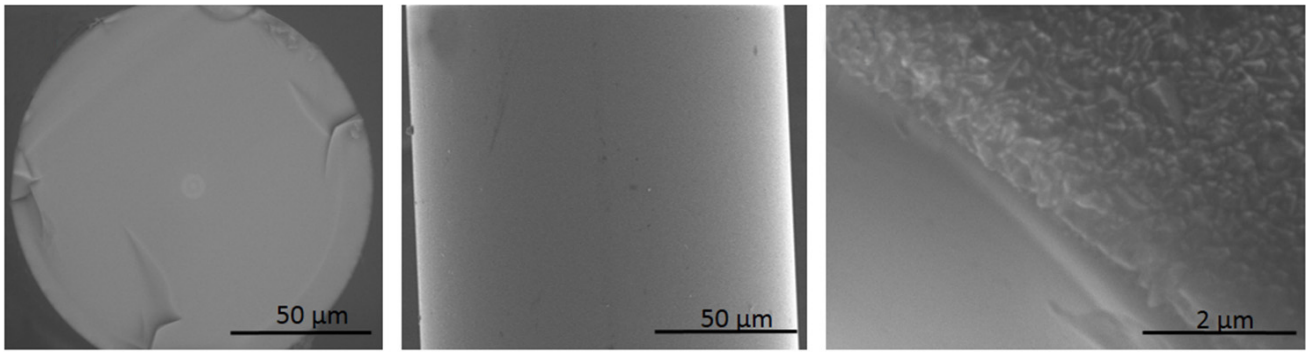

(a) (b) (c)

FIG. 2. SEM micrographs of the film, where (a) shows cross section of fiber after diamond film deposition with magnification of x1,000, (b) shows diamond layer along fiber with magnification of x1,000, and (c) B-NCD film surface with magnification of x20,000.

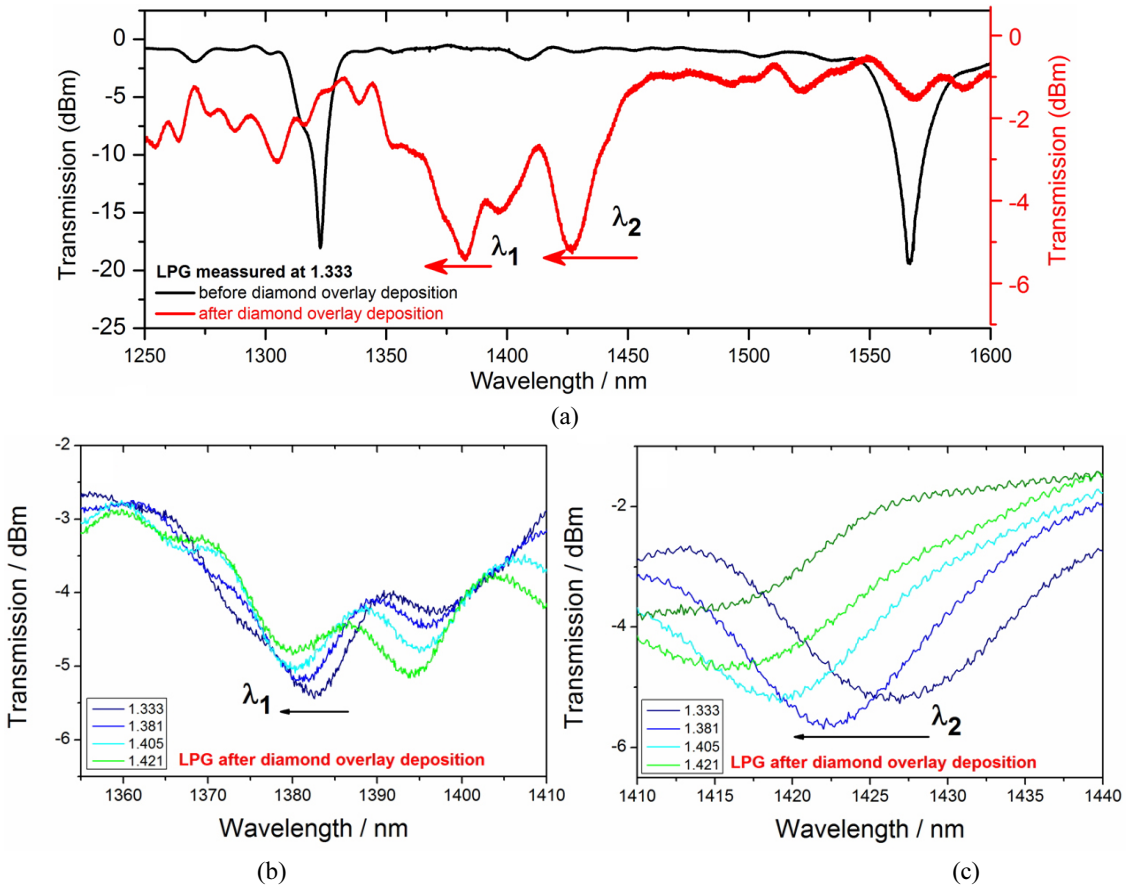

FIG. 3. Response of the LPG to variation of external RI, where (a) shows transmission spectrum before and after B-NCD deposition for grating immersed in water, (b) and (c) show selected resonance wavelength shifts λ_1 and λ_2.

reveal that fibers do not show any changes in the cladding diameter (125 μm) and fiber core diameter (~ 9 μm) due to temperature-induced stress and microwave power during the CVD process.

Moreover, an increase in external RI, which is also obtained as a result of high-*n* film deposition, induces shift of the resonances towards shorter wavelength [26]. The effect of double resonance marked in Fig. 3 as λ_1 and λ_2 is most probably a result of asymmetrical deposition of the overlay around the LPG. For asymmetrical overlay, some additional cladding modes are induced and they couple to the core mode at different wavelengths [28].

Response of LPG to dipping in several liquids with different external RI is shown in Fig. 3(b) and 3(c). For LPGs with no high-n overlays, the resonance-based spectral response disappears when external RI matches the one of the fiber cladding. When no cladding modes can be formed, no coupling takes place. In these conditions, the RI sensitivity is the highest, but the resonances are difficult to trace. In turn, the resonances are visible when external RI is lower or higher than the one of the fiber cladding. Deposition of the high-n overlay shifts appearance of this effect, i.e., vanishing of the resonances and higher sensitivity, towards lower external RI. Thin film with high-*n* modifies effective refractive index of cladding modes [28]. It can be clearly seen shift of both λ_1 and λ_2 towards shorter wavelength as a result of increase in external RI. The increase in external RI is followed by an increase in effective refractive index of cladding modes [10]. Since the resonance wavelength depends on the difference between effective refractive index of core and cladding modes, with an increase of the latter, the resonance wavelength decreases. The effect is different for λ_1 and λ_2 due to different propagation conditions (effective refractive index) of the higher order cladding modes [26]. The cladding modes induced by asymmetrical nano-overlay experience different change in their effective refractive indices when external RI changes [29]. The external RI sensitivity is 105 to 378 and 29 to 183 nm/RIU for λ_1 and λ_2 in RI range 1.33-1.41 and 1.41-1.44 RIU, respectively.

CV is considered a very useful method for investigating electrochemical properties of the material being in contact with an electrolyte. Figures 4(a) and 4(b) show the electrochemical windows and redox reaction reversibility for potassium ferricyanides solution measured with the reference microcrystalline boron-doped diamond (BDD) electrode (Fig. 4(a)) and B-NCD-coated fiber (Fig. 4(b)). It can also be seen that the electrochemical window is 2.4 times narrower than for the

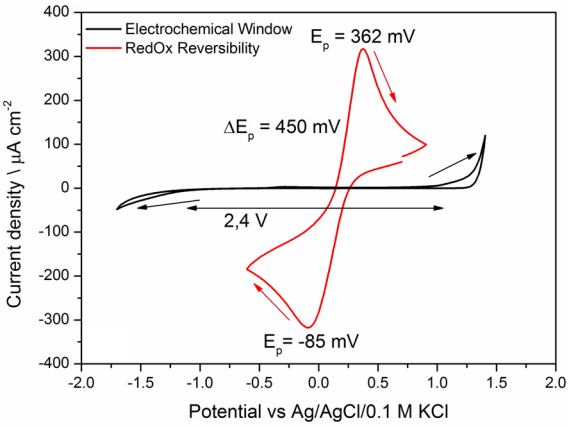

(a)

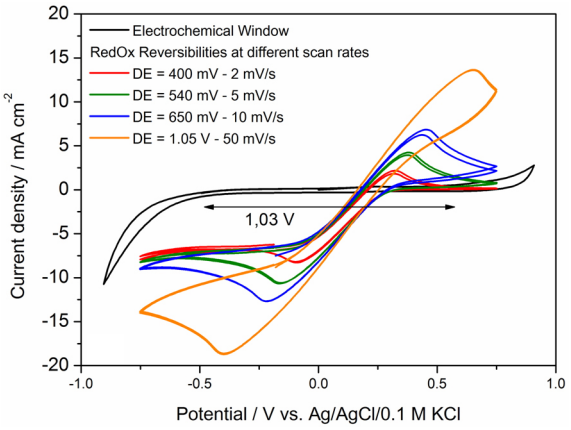

(b)

FIG. 4. Cyclic voltammograms; background current in 0.5 M Na_2SO_4 solution and reversibility of RedOx reaction of 5 nM $Fe(CN)_6^{3-/4-}$ in 0.5 M Na_2SO_4 at different scan rates obtained for (a) microcrystalline BBD reference electrode and (b) for B-NCD-coated fiber.

reference BDD film, i.e., 2.4 and 1.03 V for microcrystalline BDD and B-NCD-coated fiber, respectively. The $Fe(CN)_6^{3-/4-}$ redox system is sensitive to surface properties such as sp^2 bonded carbon or density of electronic states near the formal potential. The redox system undergoes a reversible 1-electron transfer according to the following reaction:

$$Fe(CN)_6^{3-} + e^- \Leftrightarrow Fe(CN)_6^{4-}$$

The recorded CV curves obtained for microcrystalline BDD and B-NCD-coated fiber electrodes were investigated in 5 mM $K_3Fe(CN)_6$/0.5 M $NaSO_4$ solution *vs.* Ag/AgCl/0.1 M KCl reference electrode. The recorded value of ΔE for microcrystalline BDD electrode reaches 447 mV and is two times lower than for B-NCD-coated fiber electrode ΔE = 1.05 V. However, a decreasing scan rate in the case of B-NCD-coated fiber, allows for achieving higher reversibility, up to ΔE = 400 mV at 2 mV/s. It must be emphasized that the working area, grain size and thickness of the B-NCD electrode comparing to microcrystalline BDD reference sample is significantly different and it has a strongly influence on carrier transport in the system and width of the potential window [30].

IV. CONCLUSIONS

In this work we have investigated optical and electrochemical response of optical fibers coated with B-NCD overlay. We have found that the overlay can tune response of the LPGs to variations on external refractive index and makes possible electrochemical measurements with B-NCD optical fiber. Application of electrically conductive B-NCD films allows for developing both optical and electrochemical sensing devices, and what is more, allows for combining these two capabilities in one sensing structure.

ACKNOWLEDGMENT

This work was supported by the Polish National Science Centre (NCN) under grant No. 2011/03/D/ST7/03541. The DS funds of the Faculty of Electronics, Telecommunications and Informatics at the Gdansk University of Technology under grant No. MNiD/2014/2015/1/D are also acknowledged.

REFERENCES

1. J. Dakin and B. Culshaw, *Optical Fiber Sensors: Principles and Components* (Artech House Publishers, Boston, USA, 1988).
2. A. M. Vengsarkar, P. J. Lemaire, J. B. Judkins, V. Bhatia, T. Erdogan, and J. E. Sipe, "Long-period fiber gratings as band-rejection filters," IEEE J. Lightwave Technol. **14**, 58-65 (1996).
3. M. Smietana, W. J. Bock, P. Mikulic, A. Ng, R. Chinnappan, and M. Zourob, "Detection of bacteria using bacteriophages as recognition elements immobilized on long-period fiber gratings," Opt. Express **19**, 7971 (2011).
4. M. Smietana, W. J. Bock, P. Mikulic, and J. Chen, "Tuned pressure sensitivity of dual resonant long-period gratings written in boron co-doped optical fiber," IEEE J. Lightwave Technol. **30**, 1080-1084 (2012).
5. M. Smietana, M. Koba, E. Brzozowska, K. Krogulski, J. Nakonieczny, L. Wachnicki, P. Mikulic, M. Godlewski, and W. J. Bock, "Label-free sensitivity of long-period gratings enhanced by atomic layer deposited TiO_2 nano-overlays," Opt. Express **23**, 8441-8453 (2015).
6. E. Brzozowska, M. Śmietana, M. Koba, S. Górska, K. Pawlik, A. Gamian, and W. J. Bock, "Recognition of bacterial lipopolysaccharide using bacteriophage-adhesin-coated long-period gratings," Biosens. Bioelectron. **67**, 93-99 (2015).
7. J. M. Corres, I. del Villar, I. R. Matias, and F. J. Arregui,

"Two-layer nanocoatings in long-period fiber gratings for improved sensitivity of humidity sensors," IEEE Trans. Nanotechnol. **7**, 394-400 (2008).
8. E. Davies, R. Viitala, M. Salomäki, S. Areva, L. Zhang, and I. Bennion, "Sol–gel derived coating applied to long-period gratings for enhanced refractive index sensing properties," J. Opt. Pure Appl. Opt. **11**, 015501 (2009).
9. D. Viegas, J. Goicoechea, J. M. Corres, J. L. Santos, L. A. Ferreira, F. M. Araújo, and I. R. Matias, "A fibre optic humidity sensor based on a long-period fibre grating coated with a thin film of SiO_2 nanospheres," Meas. Sci. Technol. **20**, 034002 (2009).
10. M. Smietana, J. Szmidt, M. L. Korwin-Pawlowski, W. J. Bock, and J. Grabarczyk, "Application of diamond-like carbon films in optical fibre sensors based on long-period gratings," Diam. Relat. Mater. **16**, 1374-1377 (2007).
11. M. Sobaszek, Ł. Skowroński, R. Bogdanowicz, K. Siuzdak, A. Cirocka, P. Zięba, M. Gnyba, M. Naparty, Ł. Gołuński, and P. Płotka, "Optical and electrical properties of ultrathin transparent nanocrystalline boron-doped diamond electrodes," Opt. Mater. **42**, 24-34 (2015).
12. J. Stotter, J. Zak, Z. Behler, Y. Show, and G. M. Swain, "Optical and electrochemical properties of optically transparent, boron-doped diamond thin films deposited on quartz," Anal. Chem. **74**, 5924-5930 (2002).
13. J. Stotter, S. Haymond, J. K. Zak, Y. Show, Z. Cvackova, and G. M. Swain, "Optically transparent diamond electrodes for UV-Vis and IR spectroelectrochemistry," Interface **12**, 33-38 (2003).
14. R. Bogdanowicz, M. Sobaszek, M. Ficek, M. Gnyba, J. Ryl, K. Siuzdak, and M. Śmietana, "Nanocrystalline diamond microelectrode on fused silica optical fibers for electro-chemical and optical sensing," Proc SPIE, Fifth Asia-Pacific Optical Sensors Conference **9655**, 965519 (2015).
15. M. Smietana, W. J. Bock, P. Mikulic, and J. Chen, "Increasing sensitivity of arc-induced long-period gratings-pushing the fabrication technique toward its limits," Meas. Sci. Technol. **22**, 015201 (2011).
16. R. Bogdanowicz, M. Smietana, M. Gnyba, M. Ficek, V. Stranak, L. Golunski, M. Sobaszek, and J. Ryl, "Nucleation and growth of CVD diamond on fused silica optical fibres with titanium dioxide interlayer," Phys. Status Solidi -Appl. Mater. Sci. **210**, 1991-1997 (2013).
17. I. Del Villar, C. R. Zamarreño, M. Hernaez, F. J. Arregui, and I. R. Matias, "Resonances in coated long period fiber gratings and cladding removed multimode optical fibers: a comparative study," Opt. Express **18**, 20183-20189 (2010).
18. M. Smietana, D. Brabant, W. J. Bock, P. Mikulic, and T. Eftimov, "Refractive-index sensing with inline core-cladding intermodal interferometer based on silicon nitride nano-coated photonic crystal fiber," IEEE J. Lightwave Technol. **30**, 1185-1189 (2012).
19. M. Śmietana, M. Dudek, M. Koba, and B. Michalak, "Influence of diamond-like carbon overlay properties on refractive index sensitivity of nano-coated optical fibres," Phys. Status Solidi A **210**, 2100-2105 (2013).
20. E. D. Palik, *Handbook of Optical Constants of Solids* (Academic Press, 1998).
21. P. W. May, W. J. Ludlow, M. Hannaway, P. J. Heard, J. A. Smith, and K. N. Rosser, "Raman and conductivity studies of boron-doped microcrystalline diamond, facetted nanocrystalline diamond and cauliflower diamond films," Diam. Relat. Mater. **17**, 105-117 (2008).
22. A. Zieliński, R. Bogdanowicz, J. Ryl, L. Burczyk, and K. Darowicki, "Local impedance imaging of boron-doped polycrystalline diamond thin films," Appl. Phys. Lett. **105**, 131908 (2014).
23. R. Bogdanowicz, M. Śmietana, M. Gnyba, Ł. Gołunski, J. Ryl, and M. Gardas, "Optical and structural properties of polycrystalline CVD diamond films grown on fused silica optical fibres pre-treated by high-power sonication seeding," Appl. Phys. A **116**, 1927-1937 (2014).
24. R. Bogdanowicz, "Characterization of optical and electrical properties of transparent conductive boron-doped diamond thin films grown on fused silica," Metrol. Meas. Syst. **21**, 685-698 (2014).
25. J. W. Ager III, W. Walukiewicz, M. McCluskey, M. A. Plano, and M. I. Landstrass, "Fano interference of the Raman phonon in heavily boron-doped diamond films grown by chemical vapor deposition," Appl. Phys. Lett. **66**, 616-618 (1995).
26. M. Smietana, W. J. Bock, and P. Mikulic, "Effect of high-temperature plasma-deposited nano-overlays on the properties of long-period gratings written with UV and electric arc in non-hydrogenated fibers," Meas. Sci. Technol. **24**, 094016 (2013).
27. R. Bogdanowicz, M. Sobaszek, J. Ryl, M. Gnyba, M. Ficek, Ł. Gołuński, W. J. Bock, M. Śmietana, and K. Darowicki, "Improved surface coverage of an optical fibre with nanocrystalline diamond by the application of dip-coating seeding," Diam. Relat. Mater. **55**, 52-63 (2015).
28. M. Śmietana, M. Myśliwiec, P. Mikulic, B. S. Witkowski, and W. J. Bock, "Capability for fine tuning of the refractive index sensing properties of long-period gratings by atomic layer deposited Al_2O_3 overlays," Sensors **13**, 16372-16383 (2013).
29. M. Śmietana, M. Koba, P. Mikulic, R. Bogdanowicz, and W. J. Bock, "Improved diamond-like carbon coating deposition uniformity on cylindrical sample by its suspension in RF PECVD chamber," Phys. Status Solidi A **212**, http://dx.doi.org/10.1002/pssa.201532226 (2015).
30. M. Nesládek, D. Tromson, C. Mer, P. Bergonzo, P. Hubik, and J. J. Mares, "Superconductive B-doped nanocrystalline diamond thin films: Electrical transport and Raman spectra," Appl. Phys. Lett. **88**, 232111 (2006).